Inner-shell photodetachment of C_{n}^{−} ions

N. Douguet, S. Fonseca dos Santos, and T. N. Rescigno

Phys. Rev. A **101**, 033411 — Published 23 March 2020

DOI: 10.1103/PhysRevA.101.033411

Inner-Shell Photodetachment of C_n^- Ions

N. Douguet,[1] S. Fonseca dos Santos,[2,3] and T. N. Rescigno[3]

[1]*Department of Physics, Kennesaw State University, Marietta, Georgia 30060, USA*
[2]*Department of Physics, Rollins College, Winter Park, Florida 32789 USA*
[3]*Lawrence Berkeley National Laboratory, Chemical Sciences, Berkeley, California 94720, USA*

(Dated: March 2, 2020)

We present a theoretical study of K-shell photodetachment of C_2^- and C_3^- ions. The calculations were carried out using the complex Kohn variational method. Our study addresses the recent observation that what appears as a single, narrow shape resonance close to threshold in the K-shell photodetachment of C^- splits into several peaks in the longer C_n^- carbon anion chains, with the number of peaks increasing with increasing n-values. We argue that the number of expected peaks is related to the number of symmetry-equivalent carbon atoms.

PACS numbers:

I. INTRODUCTION

Carbon anion molecules have attracted experimental and theoretical attention for many years. Bare carbon chain anions are important in combustion chemistry as intermediates in soot formation [1]. They have also been detected in interstellar space [2] and have been hypothesized to be carriers of diffuse interstellar bands [3]. Photoelectron spectroscopy has shown that carbon anions C_n^- up to $n = 9$ have linear structures while both linear and monocyclic structures are present for $10 \leq n \leq 20$ [4].

A fundamental technique for studying the structure and dynamics of negative ions is photodetachment. Early experimental studies of photodetachment were limited to removal of valence electrons, but with the advent of third-generation light sources, it has become possible to study inner-shell photodetachment from atomic and molecular anions [5, 6]. The present theoretical study was prompted by the recent observation of narrow shape resonances in the K-shell photodetachment cross sections of bare chain carbon anions up to $n = 12$ [7]. Earlier studies of K-shell photodetachment from C^- revealed a single shape resonance just above the carbon K-edge [8, 9]. The aforementioned studies indicated that this single resonance peak splits into several peaks in the carbon-chain anions, and that the number of peaks increases with the number of carbon atoms in the chain [10]. To aid in the interpretation of the experimental data and to understand the observed splitting of the shape resonance into multiple peaks in the heavier anion chains, we have carried out theoretical calculations of near-threshold K-shell photodetachment of both C_2^- and C_3^-.

The outline of this paper is as follows. In the following section, we outline the complex Kohn methodology used to compute the photodetachment cross sections. In Sec. III we present results for C_2^- and C_3^-. We conclude with a brief discussion.

II. THEORETICAL APPROACH

The calculation of photodetachment cross sections requires a description of both the initial electronic state of the molecular anion and the electron scattering wave function corresponding to the electronic state of the neutral molecule that is left behind. To produce the required continuum wave functions, we used the well-established complex Kohn variational method for electron-molecule scattering, including coupling between electronic states of the neutral fragment. Since the application of the complex Kohn method has been described in some detail previously [11, 12], only its salient features are repeated here.

In the present application, the N-electron neutral states were described by placing single core orbital vacancies in the electronic wave functions of neutral C_n. The electron-scattering wave function, with incoming boundary condition, is then expanded as:

$$\Psi^-_{\Gamma_o \ell_o m_o} = \sum_\Gamma \hat{A}(\chi_\Gamma F^-_{\Gamma\Gamma_o\ell_o m_o}) + \sum_i d_i^{\Gamma_o}\Theta_i, \qquad (1)$$

where $\hat{A}$ is the antisymmetrization operator, the first sum runs over the electronic C_n states included in the close-coupling expansion, denoted by χ_Γ, Θ_i are configuration-state functions (CSFs), and $F^-_{\Gamma\Gamma_o\ell_o m_o}$ is the corresponding photoelectron continuum function, with angular momentum quantum numbers ℓ_o and m_o for producing a neutral core-hole state Γ_o. The second sum runs over $(N+1)$-electron "penetration terms" built solely from target molecular orbitals and are included in order to relax strong orthogonality constraints between target and continuum functions [11].

In the complex Kohn method, the continuum functions are further expanded as:

$$F^-_{\Gamma\Gamma_o\ell_o m_o} = \sum_i c_i^{\Gamma\Gamma_o}\phi_i(r) + \sum_{\ell m}[f_\ell(k_\Gamma r)\delta_{\ell\ell_o}\delta_{mm_o}\delta_{\Gamma\Gamma_o} + T^{\Gamma\Gamma_o}_{\ell\ell_o m m_o} h^-_\ell(k_\Gamma r)]Y_{\ell m}(\hat{r})/r\ , \qquad (2)$$

where ϕ_i is a set of square integrable (Cartesian Gaussian) functions and f_ℓ and h^-_ℓ are partial-wave continuum

radial functions behaving asymptotically as regular and incoming Ricatti-Bessel functions, respectively:

$$\begin{aligned} f_\ell(k_\Gamma r) &\sim \frac{1}{\sqrt{k}}\sin(kr-\ell\pi/2) \\ h^-_\ell(k_\Gamma r) &\sim \frac{1}{\sqrt{k}}\exp(-i[kr-\ell\pi/2])\ . \end{aligned} \tag{3}$$

In Eqs. (1) and (2), the constants $d_i^{\Gamma_o}$, $c_i^{\Gamma\Gamma_o}$, and $T^{\Gamma\Gamma_o}_{\ell\ell_o m m_o}$, are obtained from the application of the complex Kohn variational principle [11, 12].

The matrix elements needed to construct photodetachment cross sections can be expressed in terms of the body-frame amplitudes [13]

$$\begin{aligned} I^\mu_{\Gamma_o} &= \langle\Psi_0|\mu|\Psi^-_{\Gamma_o\ell_o m_o}\rangle \\ &= \sum_{i=1}^{N+1}\int \Psi_0(r_1,,r_{N+1}) r_i^\mu \Psi^-_{\Gamma_o\ell_o m_o}(r_1,\cdots,r_{N+1}) \end{aligned} \tag{4}$$

where Ψ_0 is the initial anion wave function and r_i^μ is the dipole operator which, in the length form, is defined as:

$$r^\mu = \begin{cases} z, & \mu=0 \\ \mp(x\pm iy)/\sqrt{2}, & \mu=\pm1 \end{cases} \tag{5}$$

The integral cross section, averaged over all polarization and photoelectron directions, can be shown to take the following form [13]:

$$\sigma^{\Gamma_0} = \frac{8\pi\omega}{3c}\sum_{\ell_o m_o \mu}|I^\mu_{\Gamma_o}|^2\ . \tag{6}$$

III. COMPUTATIONAL RESULTS

From a computational viewpoint, molecular photodetachment presents some fundamental challenges. In contrast to photoionization of a neutral molecule, final state interactions in the case of molecular photodetachment are not dominated by the long-range Coulomb interaction and are thus more sensitive to short-range correlation, exchange, and polarization effects. In the cases under study, photodetachment leads to the ejection of a low-energy photoelectron and a neutral molecular radical with a core vacancy. This final-state of free electron plus radical is highly correlated and the ejected photoelectron can be either singlet or triplet coupled to the core-hole to make an overall doublet. In our calculations, some care was taken in choosing a single compact set of molecular orbitals that could accurately describe both the initial anion and final scattering states.

The square-integrable portion of the basis used in the calculations consisted of a correlation-consistent triple-zeta Gaussian basis (with f-type functions excluded) and two additional s-type and two p-type functions on each carbon atom. The scattering calculations also included numerical continuum functions up to ℓ=7.

A. C_2^- photodetachment

The spectroscopy of the C_2^- anion has been well studied [14–17]. The ground-state anion is nominally described by the configuration $1\sigma_g^2 1\sigma_u^2 2\sigma_g^2 2\sigma_u^2 1\pi_u^4 3\sigma_g$, $^2\Sigma_g^+$. Since the target anion has $^2\Sigma_g^+$ symmetry and we use the dipole approximation, we need only consider final continuum states of either $^2\Sigma_u^+$ or $^2\Pi_u$ symmetry. The hole states arising from the $1\sigma_g$ and $1\sigma_u$ orbitals are nearly degenerate and must all be included in the close-coupling expansion. Similarly, the $1\pi_u^4 3\sigma_g$ and $1\pi_u^3 3\sigma_g^2$ states are close in energy and their coupling can affect the positions and widths of the observed resonances. Therefore, eight neutral hole states were included in the coupled-channel scattering calculations:

$$\begin{aligned} &1\sigma_g 1\sigma_u^2 2\sigma_g^2 2\sigma_u^2 1\pi_u^4 3\sigma_g(^{1,3}\Sigma_g^+) \\ &1\sigma_g^2 1\sigma_u 2\sigma_g^2 2\sigma_u^2 1\pi_u^4 3\sigma_g(^{1,3}\Sigma_u^+) \\ &1\sigma_g 1\sigma_u^2 2\sigma_g^2 2\sigma_u^2 1\pi_u^3 3\sigma_g^2(^{1,3}\Pi_u) \\ &1\sigma_g^2 1\sigma_u 2\sigma_g^2 2\sigma_u^2 1\pi_u^3 3\sigma_g(^{1,3}\Pi_g) \end{aligned} \tag{7}$$

To obtain the molecular orbitals for the scattering calculations, we first performed a multi-configuration self-consistent field (MCSCF) calculation on the $^2\Sigma_g^+$ state of C_2^-. We then carried out a multi-reference configuration-interaction (MRCI) plus single-excitation calculation on the hole-states, with the restriction that no more than three electrons can be distributed over the $1\sigma_g$ and $1\sigma_u$ orbitals. The density matrices from the two lowest neutral hole states ($1\sigma_g^{-1}$ and $1\sigma_u^{-1}$) were averaged to obtain the seven natural orbitals ($1\sigma_g, 1\sigma_u, 2\sigma_g, 2\sigma_u, 1\pi_u$ and $3\sigma_g$) from which the neutral hole states were constructed.

We found no resonances of $^2\Sigma_u^+$ symmetry, so we restricted our attention to final scattering states of $^2\Pi_u$ symmetry. The cross sections from the complex Kohn calculations are obtained as a function of photoelectron energy and show a prominent $1\sigma_g \rightarrow k\pi_u$ shape resonance that peaks at 1.3 eV above the carbon K-edge. To obtain the cross section as a function of photon energy, we would need the K-edge ionization energy, which is not available from the experiments as only ions, and not photoelectrons, were detected. We therefore obtained the IP from separate, large-scale CI calculations on the C_2^- and C_2 hole states. The value we obtained was 284.1 eV, which places the calculated resonance peak at 285.4 eV. In comparing our calculated results to experiment in Fig. 1, we shifted the calculated cross section up by 0.2 eV to bring the peak into agreement with the observed results. This shift gives an implied IP of 284.3 eV. The calculated and measured results are seen to be in reasonably good agreement, with the calculated resonance profile being somewhat narrower than what is measured. This is to be expected, since the calculations were carried out at the equilibrium geometry of the anion. Accounting for nuclear motion would broaden the widths of the resonance. The calculated shoulder near 286 eV is the

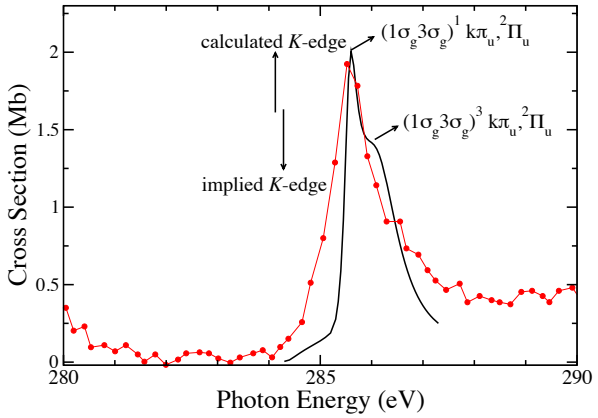

FIG. 1: Calculated cross section (solid line) for $^2\Sigma_g^+ \rightarrow ^2\,\Pi_u$ photodetachment of C_2^-. Experimental data (red dots) has been normalized to theoretical calculations. 1 Mb = 10^{-18}cm^2

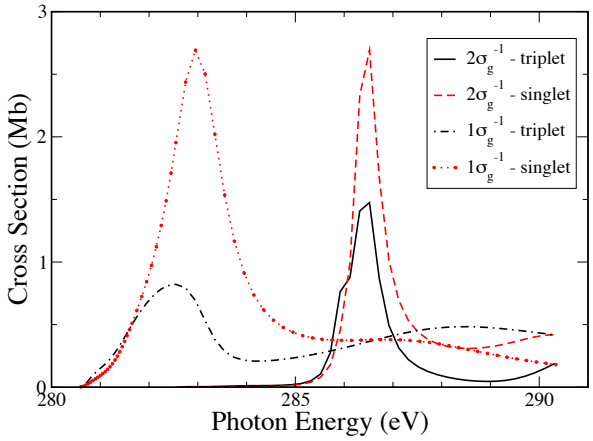

FIG. 2: Calculated cross sections for $^2\Sigma_g^+ \rightarrow ^2\,\Sigma_u^+$ photodetachment of C_3^- showing contribution of individual final channels.

shape resonance associated with the triplet hole state, which overlaps the lower singlet state resonance. Interestingly, the triplet and singlet hole-state thresholds are split by ∼0.9 eV, with the triplet state being lower in energy. Evidently, the triplet resonance lies 1.7 eV above the triplet K-shell threshold while the singlet resonance lies only 0.4 eV above its threshold.

B. C_3^- photodetachment

Additional considerations had to be addressed in the case of the C_3^- calculations. The ground state of C_3^- is nominally described by the configuration $1\sigma_g^2 2\sigma_g^2 1\sigma_u^2 3\sigma_g^2 2\sigma_u^2 4\sigma_g^2 3\sigma_u^2 1\pi_u^4 1\pi_g$, $^2\Pi_g$. In this case K-shell hole states can be made from the central carbon ($1\sigma_g^{-1}$) orbital and the two quasi-degenerate outer carbon ($2\sigma_g^{-1}$ and $1\sigma_u^{-1}$) orbitals which lie ∼2 eV higher in energy. We found that no single set of molecular orbitals could adequately describe both the central and outer carbon hole states, so we performed separate calculations on those states. The natural orbitals we used were constructed as in the C_2^- case, starting with an MCSCF calculation on the anion, followed by an MRCI plus singles calculation on the hole states, in one case doubly occupying the $2\sigma_g$ and $1\sigma_u$ orbitals and in the other case doubly occupying the $1\sigma_g$ orbital and distributing three electrons over the outer carbon $1s$ orbitals. Eleven natural orbitals ($1\sigma_g, 2\sigma_g, 1\sigma_u, 3\sigma_g, 2\sigma_u, 4\sigma_g, 3\sigma_u, 1\pi_u$ and $1\pi_g$) were extracted from the MRCI calculations and were used to form the target states in the complex Kohn calculations. The $^3\Pi_g$ target hole states were found to be split by 2.0 eV. For the central carbon scattering calculations, we performed a four channel calculation, with hole states of $^{1,3}\Pi_g$ symmetry:

$$\begin{aligned} &1\sigma_g 2\sigma_g^2 1\sigma_u^2 3\sigma_g^2 2\sigma_u^2 4\sigma_g^2 3\sigma_u^2 1\pi_u^4 1\pi_{gx}(^{1,3}\Pi_{gx}) \\ &1\sigma_g 2\sigma_g^2 1\sigma_u^2 3\sigma_g^2 2\sigma_u^2 4\sigma_g^2 3\sigma_u^2 1\pi_u^4 1\pi_{gy}(^{1,3}\Pi_{gy}) \end{aligned} \tag{8}$$

For the outer carbon scattering calculations, we did an eight channel calculation, including states of both $^{1,3}\Pi_g$ and $^{1,3}\Pi_u$ symmetry, with holes in either $2\sigma_g$ or $1\sigma_u$:

$$\begin{aligned} &1\sigma_g^2 2\sigma_g 1\sigma_u^2 3\sigma_g^2 2\sigma_u^2 4\sigma_g^2 3\sigma_u^2 1\pi_u^4 1\pi_{gx}(^{1,3}\Pi_{gx}) \\ &1\sigma_g^2 2\sigma_g 1\sigma_u^2 3\sigma_g^2 2\sigma_u^2 4\sigma_g^2 3\sigma_u^2 1\pi_u^4 1\pi_{gy}(^{1,3}\Pi_{gy}) \\ &1\sigma_g^2 2\sigma_g^2 1\sigma_u 3\sigma_g^2 2\sigma_u^2 4\sigma_g^2 3\sigma_u^2 1\pi_u^4 1\pi_{gx}(^{1,3}\Pi_{ux}) \\ &1\sigma_g^2 2\sigma_g^2 1\sigma_u 3\sigma_g^2 2\sigma_u^2 4\sigma_g^2 3\sigma_u^2 1\pi_u^4 1\pi_{gy}(^{1,3}\Pi_{uy}) \end{aligned} \tag{9}$$

The cross sections from these separate calculations were then combined, placing the central carbon $^3\Pi_g$ threshold 2.0 eV below the outer carbon $^3\Pi_g$ threshold. The calculated central carbon K-shell IP was found to be 279.89 eV. This value was shifted up by 0.66 eV so that the positions of the calculated and measured central carbon resonance peaks coincided

The calculated results are shown in Fig. 2 with the contributions from each hole-state channel displayed. As in the C_2^- case, resonances were only found in the $1,2\sigma_g \rightarrow k\pi_u$, $^2\Sigma_u^+$ channels. The total $^2\Pi_g \rightarrow ^2\,\Sigma_u^+$ cross section is compared with experiment in Fig. 3. We see that the resonance peak appears to be split into two non-overlapping contributions from the central carbon and outer carbon K-shells. Once again, the calculated results are in good agreement with experiment.

IV. DISCUSSION

Based on the results of our C_2^- and C_3^- calculations, we are in a position to explain the experimental findings

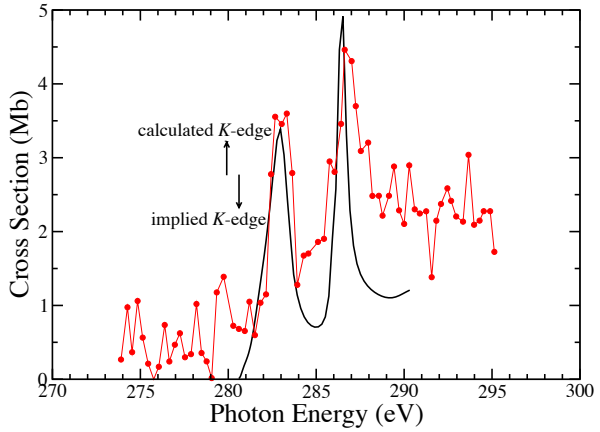

FIG. 3: As in Fig. 1, for $^2\Sigma_g^+ \rightarrow ^2\ \Sigma_u^+$ photodetachment of C_3^-.

of K-shell photoionization in the heaver carbon chain anions [10], which are displayed in Fig. 4. For every pair of symmetry-equivalent atoms there will be a pair of nearly degenerate σ_g and σ_u orbitals, from which we expect a single peak corresponding to a $\sigma_g \rightarrow k\pi_u$ resonance. The resonance peak will consist of overlapping contributions from intermediate triplet and singlet contributions that can couple with the singly occupied valence orbital to produce an overall doublet. So for the C_{2m} anions, we expect m resonance peaks. For the odd-numbered anions, there will be an additional peak coming from the central carbon $1\sigma_g$ orbital. The splitting between the peaks arises from the screening of the occupied C(1s) core orbitals which is different for the various symmetry-equivalent sites and is evidently on the order of several electron volts. So in C^-, C_2^-, C_3^-, C_4^-, C_5^-, and C_6^-, we expect 1, 1, 2, 2, 3 and 3 peaks, respectively. This observation is consistent with what is observed experimentally, although the peaks are more difficult to single out for C_5^- and C_6^-, most likely due to the molecular vibration with many degrees of freedom, but also due to the presence of cyclic structures, as pointed out in [15].

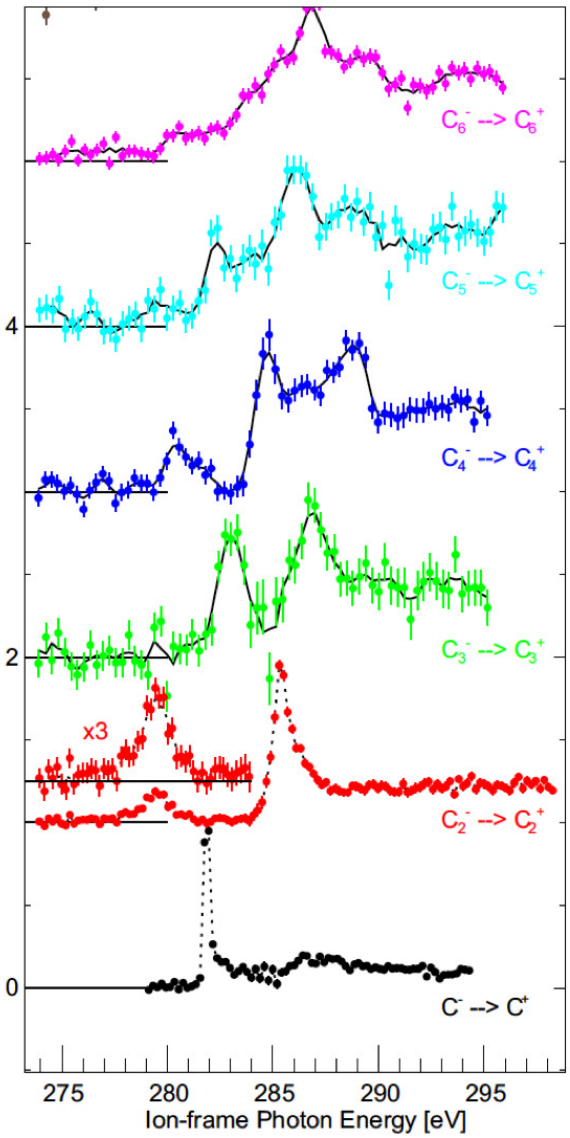

FIG. 4: K-shell photodetachment of C_n^- for n=1,6 [10]. The process is $C_n^- + \hbar\omega \rightarrow 2e^- + C_n^+$.

Acknowledgments

The authors acknowledge useful discussions with Nora Berrah and Rene Bilodeau about this work and we thank them for sharing their unpublished experimental data with us. The work performed at Lawrence Berkeley National Laboratory was supported by the U. S. Department of Energy, Office of Basic Energy Sciences, Division of Chemical Sciences, Geosciences and Biosciences under Contract No. DE- AC02-05CH11231.

[1] P. Gerhardt, S. Loffler, and K. H. Homann, Chem. Phys. Lett. **137**, 306 (1987).

[2] P. F. Bernath, K. H. Hinkle, and J. J. Kennedy, Science **244**, 562 (1989).

[3] G. A. Galazutdinov, J. Krelowski, and F. A. Musaev, Mon. Not. R. Astron. Soc. **310**, 1017 (1999).

[4] G. von Helden, P. R. Kemper, N. G. Gotts, and M. T. Bowers, Science **259**, 1300 (1993).

[5] N. Berrah, R. C. Bilodeau, I. Dumitriu, J. D. Bozek, N. D. Gibson, C. W. Walter, G. D. Ackerman, O. Zatsarinny, and T. W. Gorczyca, Phys. Rev. A **76**, 032713 (2007).

[6] N. D. Gibson, R. C. Bilodeau, C. W. Walter, D. Hanstorp, A. Aguilar, N. Berrah, D. J. Matyas, Y.-G. Li, R. M. Alton, and S. E. Lou, Journal of Physics: Conference Series **388**, 022102 (2012).

[7] R. Bilodeau, D. Gibson, W. Walter, I. Dumitriu, A. Aguilar, D. Macaluso and N. Berrah, Bull. Am. Phys. Soc. **60**, No. 7, K1.00140 (2015).

[8] N. D. Gibson, C. W. Walter, O. Zatsarinny, T. W. Gorczyca, G. D. Ackerman, J. D. Bozek, M. Martins, B. M. McLaughlin, and N. Berrah, Phys. Rev. A **67**, 030703(R) (2003).

[9] C. W. Walter, N. D. Gibson, R. C. Bilodeau, N. Berrah, J. D. Bozek, G. D. Ackerman, and A. Aguilar, Phys. Rev. A **73**, 062702 (2006).

[10] R. Bilodeau and N. Berrah, private communication.

[11] T. N. Rescigno, B. H. L. III, and C. W. McCurdy, in *Modern Electronic Structure Theory*, edited by D. R. Yarkony (World Scientific, Singapore, 1995), vol. 1, p. 501.

[12] T. N. Rescigno, C. W. McCurdy, A. E. Orel and B. H. Lengsfield III (eds. W. M. Huo and F. A. Gianturco, Plenum, New York, 1995), p. 1.

[13] T. N. Rescigno, B. H. Lengsfield, and A. E. Orel, J. Chem. Phys. **99**, 5097 (1993).

[14] W. C. Lineberger and T. A. Patterson, Chem. Phys. Lett. **13**, 40 (1972).

[15] D. W. Arnold, S. E. Bradforth, T. N. Kitsopoulos, and D. M. Neumark, J. Chem Phys. **95**, 8753 (1991).

[16] P. L. Jones, R. D. Mead, B. E. Kohler, S. D. Rosner, and W. C. Lineberger, The Journal of Chemical Physics **73**, 4419 (1980).

[17] S. Gerber, J. Fesel, M. Doser, and D. Comparat, New Journal of Physics **20**, 023024 (2018).